Van der Waals Interaction between Two Crossed Carbon Nanotubes

Alexander I. Zhbanov,[†,‡] Evgeny G. Pogorelov,[†,*] and Yia-Chung Chang[†]

[†]Research Center for Applied Sciences, Academia Sinica, 128, Section 2, Academia Road Nankang, Taipei 115, Taiwan, and [‡]Department of Mechatronics, Gwangju Institute of Science and Technology (GIST), 1 Oryong-dong, Buk-gu, Gwangju, 500-712, Korea

ABSTRACT The analytical expressions for the van der Waals potential energy and force between two crossed carbon nanotubes are presented. The Lennard-Jones potential between pairs of carbon atoms and the smeared-out approximation suggested by L. A. Girifalco (*J. Phys. Chem.* 1992, *96*, 858) were used. The exact formula is expressed in terms of rational and elliptical functions. The potential and force for carbon nanotubes were calculated. The uniform potential curves for single- and multiwall nanotubes were plotted. The equilibrium distance, maximal attractive force, and potential energy have been evaluated.

KEYWORDS: carbon nanotubes · van der Waals interaction · Lennard-Jones potential · smeared-out approximation · equilibrium distance

The van der Waals (VDW) interaction plays very important role in nano-electromechanical systems and nanoelectronic devices.[1,2] Carbon nanotubes (CNTs) are promising materials for creating nanotweezers,[3] nanoswitches,[4] bearings,[5] nanotube random access memory,[6,7] and gigahertz nano-oscillators,[8] *etc.* The VDW forces are very critical for understanding the growth mechanism of fullerenes and nanotubes and formation process of ropes and bundles. Potentials for graphite layers,[9] two fullerenes,[10] fullerene and surface,[11] nanotube and surface,[12] and fullerenes inside and outside of nanotubes[13] are well studied. There are a number of publications devoted to the interaction between the inner and the outer parallel tubes such as single-wall (SWNTs),[13−17] double-wall (DWNTs),[17−19] and multiwall nanotubes (MWNTs).[20,21]

The present work is dedicated to the interplay between two CNTs crossed at an arbitrary angle. Frequently studies of CNT systems have assumed that the VDW potential energy can be approximated by a sum of two-body interactions between pairs of carbon atoms.

The interaction between a pair of neutral atoms or molecules involves both short-range and long-range interactions. A repulsive force at short ranges is the result of the electron exchange (due to Pauli exclusion principle). An attractive force at long ranges or the van der Waals force is electromagnetic in origin. As was first shown by London (1930),[22] it arises from the second-order perturbation theory applied to the electrostatic dipole−dipole interaction.

Many body effects are very important for the interaction between clusters consisting of many atoms. The problem of the many-body character of the VDW potential is discussed for example in refs 23 and 24. The many-body corrections of the VDW potential have been derived for CNT bundles and phases of various gases.[25] Mainly the three-body energy based on the Axilrod−Teller−Muto expression[26,27] was used in references above.

A more accurate approximation is given by the Lifshitz or Casimir formulation. If the separation between two atoms is sufficiently large then the retardation of the electromagnetic fluctuating interaction contributes significantly. The interaction of atoms taking retardation into account was considered by Casimir (1948)[28,29] and Lifshitz (1956).[30,31]

Casimir's theory describes the interaction between two atoms or an atom and a flat surface of a macrobody. Usually it is referred to as the Casimir−Polder force.[29] The general theory of the van der Waals forces based on the concept of a frequency-dependent dielectric permittivity was developed by Dzyaloshinskii, Lifshitz, and Pitaevskii.[31]

The Casimir or Lifshitz theory was successfully applied for calculation of VDW energy between CNT bundles and microparticles.[17] The application of the Casimir or Lifshitz theory to the CNTs causes serious

*Address correspondence to evgeny@gate.sinica.edu.tw.

Received for review April 9, 2010 and accepted September 09, 2010.

Published online September 23, 2010.
10.1021/nn100731u

problems because their boundary surface is not flat and SWNTs are not characterized by the macroscopic concept of a frequency-dependent dielectric permittivity.[32]

There are many different approaches based on the density functional theory (DFT) that allow the study of the cohesive and adsorption properties of SWNTs and CNT bundles arising from the VDW interactions.[33] The time-dependent (TD) DFT provides a better description than the usual DFT for the attractive part of the VDW potential. However DFT or TD-DFT is known to be reliable in describing short-range electron correlation effects; their accuracy decreases rapidly for distances greater than about 15% beyond the equilibrium distance. Several newly developed approaches which partially overcome this defect are based on adding certain damped potentials (DFT-D method).[34−36] Problems related with the application of DFT calculations to CNTs are discussed for example in refs 16, 37, and 38.

The empirical approach based on the pairwise summation of interatomic Lennard-Jones (LJ) potentials adapted for graphitic structures has also been widely applied. To evaluate the potential between two crossed SWNTs or MWNTs, in the present work we apply the pairwise summation of adapted LJ potentials and the method of the smeared-out approximation suggested by L.A. Girifalco[10,38] for fullerene molecules and for CNTs. The model potentials for the VDW interaction are based on empirical functions whose parameters are obtained from empirical fits to properties of the relevant CNT systems. Despite its simplicity this model was very successful in the description of many complicated technological problems such as the gigahertz oscillation of DWNTs,[39] wave propagation,[40] and stability[41] in the deformed nanotubes.

It was shown by Ruoff *et al.*[42] that VDW forces between adjacent nanotubes can deform them, destroying cylindrical symmetry. Using molecular mechanics Hertel *et al.*[43] calculated radial deformations of carbon nanotubes adsorbed on surface. The radial compressions of adsorbed SWNTs with respect to the undistorted free tubes do not exceed 2% for a tube diameter of 13.5 Å and smaller. When the number of inner shells is greater than 8, the compressions are less than 1% for 54.3 Å MWNT. Experimental observations of a bundle of two SWCNTs show that the deformation does not exceed 4% for 21 Å and smaller SWNTs.[44,45] Therefore we can apply the continuum medium model for SWNTs with small radius and MWNTs consisting of many inner shells. The other reasons for using the Girifalco model in the present work are its simplicity and the sufficient level of accuracy. The next advantage is that the final potential can be written in analytical form.

The close conformity of the potential shape between DFT calculations and the pairwise integration lends support for the validity of Girifalco method. Amovilli and March[46] found a good agreement between VDW potentials for parallel CNTs predicted by DFT and the Girifalco model. Pacheco and Ramalho[33] used LDA for distances near and less than the equilibrium separation and a multipole expansion for the longer range distances of $C_{60}-C_{60}$ interaction. The two potentials are close to each other in the vicinity of minimum and beyond. Both potentials reproduce the experimental behavior-of-state up to at least 5000 atm. Thus we conclude that the Girifalco model with constants depending on the structure of interacting objects may be accurate enough for distances between objects in the vicinity of equilibrium.

It is remarkable that empirical parameters have been so successful in providing a unified, consistent description of the properties that depend on the weak interactions between and among graphene sheets, fullerene molecules, and nanotubes.[38]

MODEL

The LJ potential for two carbon atoms in graphene−graphene structure is

$$\varphi(r) = -\frac{A}{r^6} + \frac{B}{r^{12}} \tag{1}$$

where r is a distance, $A = 15.2$ eV·Å^6 and $B = 24100$ eV·Å^{12} are the attractive and repulsive constants, respectively.[13] Following Girifalco[10] we approximate the potential between two crossed SWNTs by integration of the LJ potential

$$\varphi_{tt} = \nu^2 \int \varphi(r)\, d\Sigma_1\, d\Sigma_2 \tag{2}$$

The mean surface density of carbon atoms for a hexagonal structure is

$$\nu = \frac{4}{3\sqrt{3}a_1^2} \approx 0.393 \text{ atoms per Å}^2 \tag{3}$$

where $a_1 = 1.42$ Å is the observed value of the C−C bond length for periodic graphite.[18] If we know VDW interaction between two SWNTs then according to the Girifalco approach we may obtain the interaction between MWNTs by summation over all pairs of layers.[20]

RESULTS AND DISCUSSION

We have studied the VDW interaction between two crossed CNTs by using the continuum LJ approximation. We have performed the analytical integrations for the potential energy of interaction between two CNTs crossed at an arbitrary angle. Schematic illustrations of interaction between SWNT and chain of carbon atoms and between two MWNTs are given in Figure 1.

It is clear from eqs 17, 26, 29, and 36 (see Methods section) that the potential energy and VDW force is inversely proportional to the sine of angle γ between two tubes. For the right angle case, the energy and the attractive force are minimal. If the angle is infinitesimal then energy and force approaches infinity. We use the

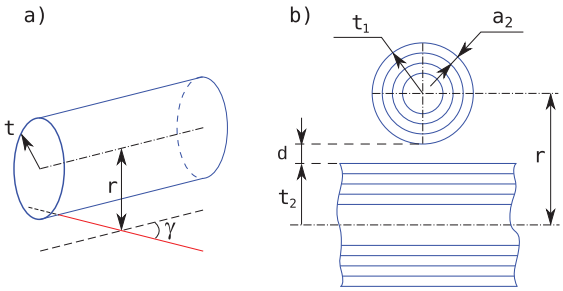

Figure 1. Schematic drawing of interaction between (a) SWNT and line and (b) two MWNTs.

parameter $d = r - t_1 - t_2$ to characterize the distance between tubes. From eq 17 we see that the equilibrium distance $d_0 = d_0(t_1, t_2)$ does not depend on angle γ but only on radii of tubes t_1 and t_2. Also the potential well φ^0_{tt} is inversely proportional to $\sin\gamma$. Therefore, we assume in all our following illustrations and tables for both SWNTs and MWNTs that nanotubes are crossed at a right angle.

The analytical integrations for the potential energy of interaction between two identical SWNTs are plotted in Figure 2. On the basis of the results illustrated in Figure 2, it can be concluded that the real gap between surfaces of interacting SWNTs of different radii in an equilibrium state is changed only slightly in the range $d_0 = 2.92-2.93$ Å. We have carried out many calculations with different radii t_1 and t_2. The equilibrium distance is practically independent of tube radius and totally independent of angle γ. Very weak dependence of equilibrium gap from radii of parallel tubes has been mentioned in refs 14, 20, and 28.

For comparison, in ref 10 the equilibrium gap between two fullerenes C_{60} is given as 2.95 Å, while the equilibrium distance between two parallel nanotubes is in the range 3.11−3.17 Å.[14,20,38] We see that a certain jump is observed at the transition from crossed to parallel configuration. This is due to the fact that in the central parts of crossed tubes the nearest surfaces repel each other while the far-separated surfaces attract each other, but for the distant parts of crossed tubes all surfaces attract each other. In the parallel case we have the VDW interaction similar to which happens in the central parts of crossed tubes, but we do not have attracting distant parts. Unfortunately we cannot compare the well depth for crossed and parallel tubes because in the crossed case the well depth is measured in eV, while for parallel tubes the units should be eV per unit length.

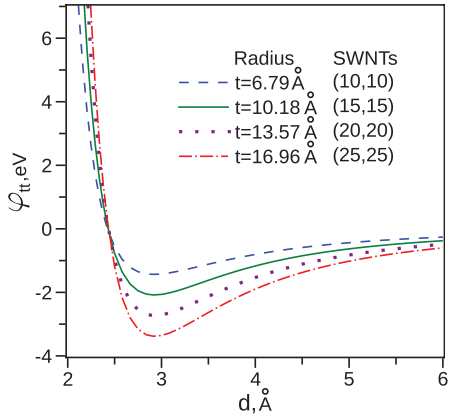

Figure 2. Potential energies for interaction between pairs of identical SWNTs, $\gamma = \pi/2$.

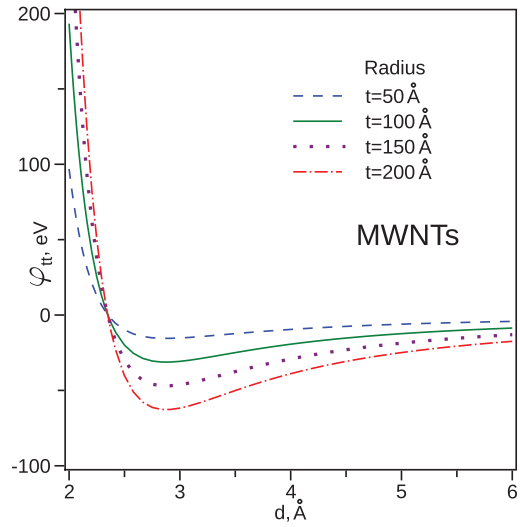

Figure 3. Potential energies for interaction between pairs of MWNTs of equivalent size. MWNTs contain 11 layers, $\gamma = \pi/2$.

In the case of MWNT interaction we assume that each pair of layers interacts as SWNTs and use summation over all pairs. The potential energy for two MWNTs of equivalent radii is plotted in Figure 3. In these calculations we assume that each MWNT consists exactly of 11 walls. The equilibrium distance between their surfaces is found to be $d_0 = 2.87$ Å, which is smaller than the equilibrium SWNT−SWNT gap.

From our calculations it follows that only several outer shells of MWNTs play an essential role in the VDW interaction. For example, if two equal MWNTs with $d = 200$ Å contain 6, 11, 16, 21, or 26 layers, then the minimum energy is −60.78, −62.77, −63.48, −63.83, or −64.03 eV. The dependence of the minimum potential energy from the number of inner layers for pairs of equivalent MWNTs is presented in Table 1.

It was found that the VDW interaction between $C_{60}-C_{60}$, C_{60}−SWNT, C_{60}−graphene, graphene−graphene, parallel SWNT−SWNT, and parallel MWNT−MWNT can be described by a universal

TABLE 1. Dependence of Potential Well $|\varphi^0_{tt}|$ (eV) from Number of Layers (6, 11, 16, 21, 26) for MWNTs of Equivalent Radii, $\gamma = \pi/2$

radius (Å)	6	11	16	21	26
50	15.09	15.48	N/A	N/A	N/A
100	30.31	31.25	31.56	31.70	31.75
150	45.55	47.01	47.52	47.76	47.90
200	60.78	62.77	63.48	63.83	64.03

TABLE 2. Calculated Depth $|\varphi^0_{tt}|$ (eV) for SWNTs (Upper-Right Side) and Approximation (Lower-Left Side), $\gamma = \pi/2$

radius (Å)	6.79	10.18	13.57	16.96
6.79	1.426\1.434	1.728	1.979	2.202
10.18	1.723	2.080\2.081	2.384	2.653
13.57	1.975	2.385	2.734\2.731	3.039
16.96	2.199	2.655	3.043	3.388\3.382

TABLE 3. Calculated Depth $|\varphi^0_{tt}|$ (eV) for MWNTs Consisting of 11 Shells (Upper-Right Side) and Approximation (Lower-Left Side), $\gamma = \pi/2$

radius (Å)	50	100	150	200
50	15.45\15.48	21.99	26.97	31.17
100	21.95	31.20\31.25	38.33	44.29
150	26.93	38.27	46.95\47.01	54.32
200	31.12	44.23	54.25	62.70\62.77

curve.[13,14,20] In our case universal curve means that a plot of $\bar{\varphi}_{tt} = \varphi_{tt}/|\varphi^0_{tt}|$ against $\bar{d} = d/d_0$ gives the same curve for all tube−tube interactions, where φ^0_{tt} is the minimum energy and d_0 is the equilibrium spacing for the two crossed tubes. As pointed above, the equilibrium distances are approximately constants for SWNTs and MWNTs with fixed number of shells.

We have calculated the minimum energy φ^0_{tt} for SWNTs of different radii (Table 2) as well as for MWNTs (Table 3). The function $\varphi^0_{tt}(t_1, t_2)$ is symmetric, so we look over different simple symmetric functions to fit it. These results can be described very well as can be seen in Figure 4 by the approximating formula

$$\varphi^0_{tt} \approx \varphi^0_{CNT}(t_1, t_2, \gamma) = \frac{\nu^2}{\sin\gamma}\left(C_1^{CNT}\sqrt{t_1 t_2} + C_2^{CNT}\frac{t_1 + t_2}{\sqrt{t_1 t_2}}\right) \quad (4)$$

where $C_1^{SWNT} = -1.3232$ eV Å^3, $C_2^{SWNT} = -0.4012$ eV Å^4, and $C_1^{MWNT} = -2.161$ eV Å^3, $C_2^{MWNT} = 1.036$ eV Å^4 are parameters for SWNTs and MWNTs with 11 shells, respectively. It can be figured out from Tables 2 and 3 that the approximating formula gives very good accuracy.

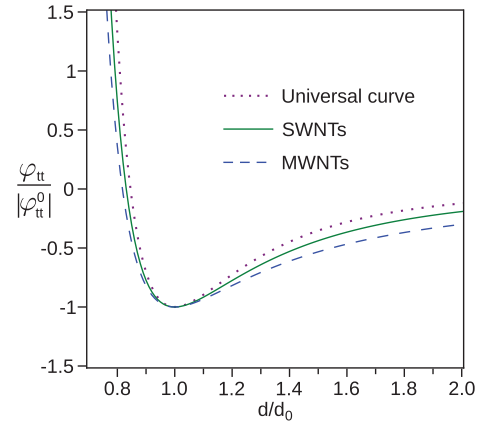

Figure 5. Uniform potential for SWNTs and MWNTs with 11 shells of arbitrary sizes. Dotted line is the universal curve suggested by L.A. Girifalco *et al.*; angle γ is arbitrary.

It is remarkable that plots for CNTs of different radii crossed at an arbitrary angle fall on the same uniform curve with accuracy within the line thickness. Using dimensionless potential $\bar{\varphi}_{tt}$ we can fit the potential of interaction between pairs of different SWNTs to one uniform curve and between pairs of different MWNTs with 11 shells to another one (in Figure 5). Actually if the number of shells is bigger than 11 the uniform curves are practically the same. For comparison Figure 5 also shows a universal potential suggested by Girifalco L.A. *et al.*[13]

We try to approximate the uniform curve $\bar{\varphi}_{tt}(\bar{d})$ by $\bar{\varphi}_s(\bar{d})$ for SWNTs and by $\bar{\varphi}_m(\bar{d})$ for MWNTs with 11 shells in the form

$$\bar{\varphi}_i(\bar{d}) = \frac{b_i}{\bar{d}^{n_i}} - \frac{c_i}{\bar{d}^{m_i}}, \quad n_i > m_i \quad (5)$$

where $i = s$ for SWNTs and $i = m$ for MWNTs with 11 shells. When $\bar{d}$ is changed in the region from 0.01 to 0.6, the main influence comes from the first term, and using logarithm scale we may find that $n_i = 9$, $b_s = 0.49$, $b_m = 0.3$. From the conditions

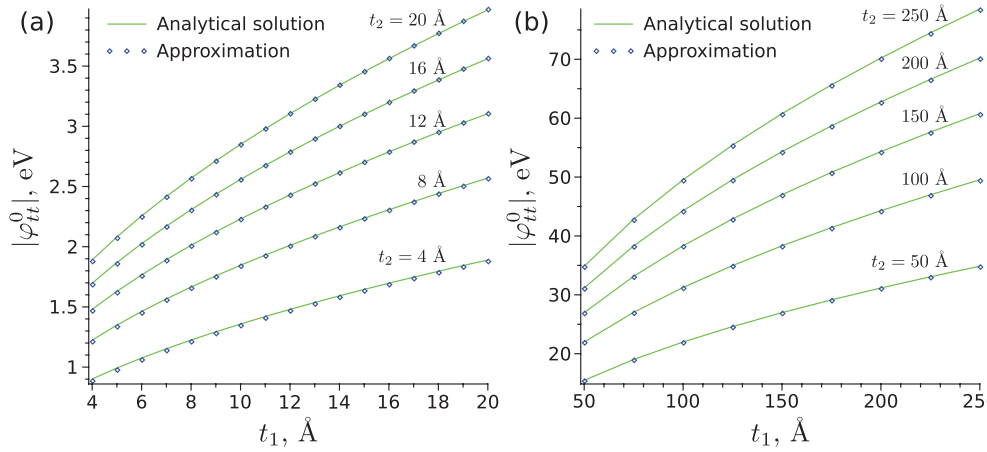

Figure 4. Calculated depth $|\varphi^0_{tt}|$, eV eq 17 and approximation eq 4 (a) for SWNTs and (b) for MWNTs consisting of 11 shells, $\gamma = \pi/2$.

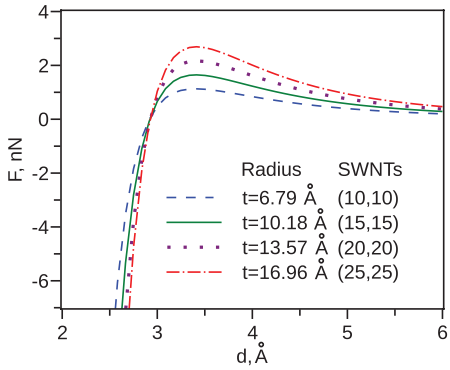

Figure 6. van der Waals forces between two identical SWNTs, $\gamma = \pi/2$.

$$\bar{\varphi}_i(1) = -1, \quad \frac{\partial \bar{\varphi}_i}{\partial \bar{d}}(1) = 0 \tag{6}$$

we find that

$$\bar{\varphi}_i(\bar{d}) = b_i\left(\frac{1}{\bar{d}^9} - \frac{b_i + 1}{b_i}\frac{1}{\bar{d}^{9b_i/(b_i+1)}}\right) \tag{7}$$

This approximation works very well for $\bar{d}$ in the region from 0.01 to 5.

Now using eqs 4 and 7 we can write an approximation for the VDW potential according to the method of uniform curve. For SWNTs we have

$$\varphi(d, t_1, t_2, \gamma) \approx \varphi^0_{SWNT}(t_1, t_2, \gamma)\,\bar{\varphi}_s(d/d_0), \quad d_0 = 2.925 \text{ Å} \tag{8}$$

and for MWNTs with 11 shells

$$\varphi(d, t_1, t_2, \gamma) \approx \varphi^0_{MWNT}(t_1, t_2, \gamma)\,\bar{\varphi}_m(d/d_0), \quad d_0 = 2.87 \text{ Å} \tag{9}$$

Figures 6 and 7 show the forces for two CNTs of equivalent radii. As we see in these figures the behavior for both SWNTs and MWNTs with 11 shells is qualitatively similar. The distance where the attractive force reaches its maximum is in the range 3.40−3.41 for SWNTs and it is practically constant, 3.36 Å, for MWNTs.

CONCLUSIONS

We used Lennard-Jones potential between two carbon atoms and apply the smeared-out approximation suggested by L.A. Girifalco to calculate the interaction between two crossed CNTs of different diameters. The exact formulas for potential energy and van der Waals forces are expressed in terms of rational and elliptical functions. These formulas become much simpler in the case of interaction between equivalent tubes. We evaluated the equilibrium distance, maximal attractive force and potential energy for SWNTs and MWNTs.

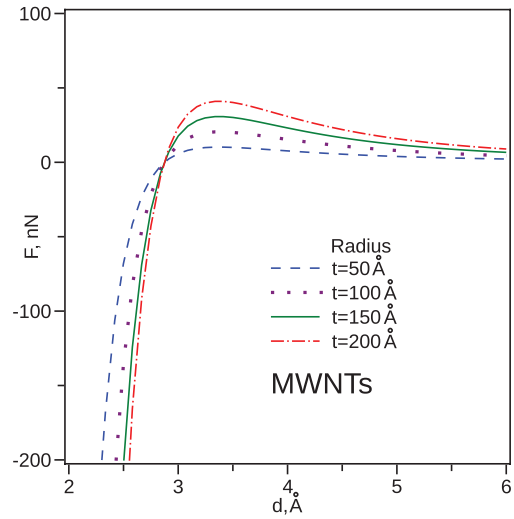

Figure 7. van der Waals force between pairs of MWNTs of equivalent size. MWNTs contain 11 layers, $\gamma = \pi/2$.

It is remarkable that the optimal distance d_0 does not depend on the angle γ between two straight tubes and is almost constant for CNTs of different radii. The equilibrium distance for crossed SWNTs is 2.93 Å. For comparison[14] the equilibrium gap between two parallel SWNTs is 3.15 Å. The optimal distance for MWNTs is smaller than that for SWNTs. The presence of additional layers makes the optimal distance smaller.

We also found that within very good accuracy the potential well φ_0 can be well approximated by a linear combination of $(t_1t_2)^{1/2}$ and $(t_1 + t_2)/(t_1t_2)^{1/2}$, where t_1 and t_2 are the radii of CNTs. Thus the value of φ_0 can be evaluated without any integration.

We found that if the energy is expressed in units of the well depth φ_0 and the distance is measured in the equilibrium VDW gap d_0, as suggested by Girifalco *et al.*, then all the potentials between two arbitrary SWNTs fall on the same uniform curve, and all the potentials between two arbitrary MWNTs with fixed number of layers fall on another uniform curve. On the basis of the uniform curves and expressions for φ_0 the VDW potential function for any two CNTs can be easily reproduced.

The uniform curve for SWNT interaction does not depend on VDW constants A and B taken in reasonable physical diapason. For a uniform curve of MWNT interactions we observed very small dependence on constants A and B. Using the method of uniform curve we also obtained a simple approximate formula for the VDW potential $\varphi(d, t_1, t_2, \gamma)$.

METHODS

Ancillary Integrals. To calculate the VDW interaction between two nanotubes we have to use a few useful integrals. For the integral of LJ potential between two straight lines

$$I_{ij}(r) = \int \varphi(r)\, dl_1\, dl_2, \tag{10}$$

we obtain

$$I_{ll}(r) = \frac{\pi}{\sin\gamma}\left(-\frac{A}{2r^4} + \frac{B}{5r^{10}}\right) \quad (11)$$

where γ is the angle and r is the distance between the two lines, and index ll means "line−line". For the next integral between a line and a tube we have

$$I_{lt}(r, t) = t\int_{-\pi}^{\pi} I_{ll}(r - t\sin\beta)\, d\beta, \quad r > t \quad (12)$$

where t is tube radius, r is distance between the line and the axis of the tube, and index lt means "line−tube". Figure 1a illustrates the schematic image of SWNT and line. Introducing a new variable $u = \tan(\beta/2)$ and using the method of partial fractions we get

$$I_{lt}(r, t) = \frac{1}{\sin\gamma}\left(-\frac{A\cdot x^3 G_A(x)}{2r^3} + \frac{B\cdot x^9 G_B(x)}{5r^9}\right) = \frac{1}{\sin\gamma}\left(-\frac{A\cdot G_A(x)}{2t^3} + \frac{B\cdot G_B(x)}{5t^9}\right) \quad (13)$$

where

$$x \equiv \frac{r}{t}, \quad G_A(x) = \frac{\pi^2 x(2x^2 + 3)}{(x^2 - 1)^{7/2}}$$

$$G_B(x) = \frac{\pi^2 x(128x^8 + 2304x^6 + 6048x^4 + 3360x^2 + 315)}{64(x^2 - 1)^{19/2}}$$

Tube−Tube Interaction Potential. Figure 1b schematically illustrates the interaction between two MWNTs crossed at right angle for convenience but hereinafter we consider tubes crossed at arbitrary angle γ. Parameter $a_2 = 3.44$ Å is the average distance between two layers in MWNTs;[18] d is the gap between tubes.

In a particular case these tubes may consist only of one layer. We note t_1 as a radius of the first SWNT and t_2 as a radius of the second one ($r = d + t_1 + t_2$). The interaction potential between two SWNTs is

$$\varphi_{tt}(r, t_1, t_2) = 2\nu^2\int_{r-t_2}^{r+t_2} I_{lt}(x, t_1)\sqrt{1 + y'^2(x)}\, dx \quad (14)$$

where $y(x) = (t_2^2 - (x - r)^2)^{1/2}$, index tt means "tube−tube".

Introducing dimensionless parameters

$$x = \frac{x}{t_1}, \quad b_1 = \frac{r}{t_1}, \quad b_2 = \frac{r}{t_2}, \quad k = \frac{t_2}{t_1} \quad (15)$$

and using eq 13 we have

$$\varphi_{tt}(r, t_1, t_2) = \nu^2 t_1\int_{b_1-k}^{b_1+k} \frac{2kI_{lt}(x, t_1)}{\sqrt{k^2 - (x - b_1)^2}}\, dx \quad (16)$$

After some transformations we write

$$\varphi_{tt}(r, t_1, t_2) = \frac{\nu^2}{\sin\gamma}\left(-\frac{A\cdot g_A}{r^2} + \frac{B\cdot g_B}{r^8}\right) \quad (17)$$

where multipliers for attractive and repulsive terms are

$$g_A(b_1, b_2) = \frac{b_1^2}{2}\int_{b_1-k}^{b_1+k} \frac{2kG_A(x)}{\sqrt{k^2 - (x - b_1)^2}}\, dx \quad (18)$$

$$g_B(b_1, b_2) = \frac{b_1^8}{5}\int_{b_1-k}^{b_1+k} \frac{2kG_B(x)}{\sqrt{k^2 - (x - b_1)^2}}\, dx \quad (19)$$

The obtained eq 18 and eq 19 represent the elliptic integrals. In modern mathematics elliptic integral is defined as integral $\int R(x, y)\, dx$, where $R(x, y)$ is rational function of x and y, and y^2 is a cubic or quartic polynomial in x. With the appropriate reduction formula every elliptical integral can be expressed in terms of elementary functions and canonical elliptic integrals of first, second, and third kind. The method of integration is quite complicated but well-known.[47−50] We would like to present only the final answer. For the attractive part we have the dimensionless parameter

$$g_A = g_{AK}(b_1, b_2)K(h) + g_{AE}(b_1, b_2)E(h) \quad (20)$$

where

$$h = \frac{2\sqrt{b_1 b_2}}{\sqrt{(b_1 b_2 + b_1 - b_2)(b_1 b_2 + b_2 - b_1)}} \quad (21)$$

Analogically for the repulsive part we write the dimensionless parameter

$$g_B = g_{BK}(b_1, b_2)K(h) + g_{BE}(b_1, b_2)E(h) \quad (22)$$

Details of the definition of dimensionless coefficients $g_{AK}(b_1, b_2)$, $g_{AE}(b_1, b_2)$, $g_{BK}(b_1, b_2)$, and $g_{BE}(b_1, b_2)$, are given in the Appendix.

As we can see, the final result eq 17 is quite large but it works much better than the usual numerical integration, because this analytical formula provides high accuracy and high speed of calculations.

Tube−Tube Force. The resulting force caused by VDW interaction is

$$F(r) = -\frac{d\varphi_{tt}(r)}{dr} \quad (23)$$

Using the expressions[48]

$$\frac{dK(x)}{dx} = \frac{E(x)}{(1 - x^2)x} - \frac{K(x)}{x} \quad (24)$$

and

$$\frac{dE(x)}{dx} = \frac{1}{x}(E(x) - K(x)) \quad (25)$$

it is possible to obtain the analytical formula for the VDW force. After the usual differentiation over r we have

$$F(r, t_1, t_2) = \frac{\nu^2}{\sin\gamma}\left(-\frac{Af_A}{r^3} + \frac{Bf_B}{r^9}\right) \quad (26)$$

where

$$f_A = f_{AK}(b_1, b_2)K(h) + f_{AE}(b_1, b_2)E(h) \quad (27)$$

$$f_B = f_{BK}(b_1, b_2)K(h) + f_{BE}(b_1, b_2)E(h) \quad (28)$$

The definition of dimensionless coefficients $f_{AK}(b_1, b_2)$, $f_{AE}(b_1, b_2)$, $f_{BK}(b_1, b_2)$, and $f_{BE}(b_1, b_2)$ are given in the Appendix.

Potential and Force between Equivalent Tubes. The potential and force can be more simply expressed in the case when the radii of interacted tubes are equal, $t_1 = t_2 = t$; therefore, $b_1 = b_2 = b = r/t$. Then we have, for the potential,

$$\varphi_{tt}^*(r, t) = \frac{\nu^2}{\sin\gamma}\left(-\frac{Ag_A^*}{r^2} + \frac{Bg_B^*}{r^8}\right) \quad (29)$$

where

$$g_A^* = g_{AK}^* K(2/b) + g_{AE}^* E(2/b) \quad (30)$$

$$g_B^* = g_{BK}^* K(2/b) + g_{BE}^* E(2/b) \quad (31)$$

and

$$g^*_{AK} = -\frac{2\pi^2(5b^2 - 4)}{3(b^2 - 4)^2} \quad (32)$$

$$g^*_{AE} = \frac{2\pi^2(32 - 20b^2 + 11b^4)}{3(b^2 - 4)^3} \quad (33)$$

$$g^*_{BK} = -\pi^2(4609b^{14} + 56038b^{12} + 321132b^{10} - 473632b^8 + 1885952b^6 - 3867648b^4 + 4510720b^2 - 2293760)/(1575(b^2 - 4)^8) \quad (34)$$

$$g^*_{BE} = \pi^2(7129b^{16} + 97220b^{14} + 763489b^{12} - 1533424b^{10} + 7790944b^8 - 21756160b^6 + 38781184b^4 - 40099840b^2 + 18350080)/(1575(b^2 - 4)^9) \quad (35)$$

Similarly, in the case of $t_1 = t_2$ for the force we have

$$F^*(t, r) = \frac{\nu^2}{\sin\gamma}\left(-\frac{Af^*_A}{r^3} + \frac{Bf^*_B}{r^9}\right) \quad (36)$$

$$f^*_A = \frac{4\pi^2}{3(b^2 - 4)^4}\left(f^*_{AK}K\left(\frac{2}{b}\right) + f^*_{AE}E\left(\frac{2}{b}\right)\right) \quad (37)$$

$$f^*_B = \frac{\pi^2}{315(b^2 - 4)^{10}}\left(f^*_{BK}K\left(\frac{2}{b}\right) + f^*_{BE}E\left(\frac{2}{b}\right)\right) \quad (38)$$

$$f^*_{AK} = 13b^6 - 62b^4 + 64b^2 - 96 \quad (39)$$

$$f^*_{AE} = -25b^6 + 36b^4 - 176b^2 + 192 \quad (40)$$

$$f^*_{BK} = 9722b^{18} + 129650b^{16} + 537641b^{14} - 5804036b^{12} + 11418976b^{10} - 50923136b^8 + 118211840b^6 - 180548608b^4 + 162971648b^2 - 66060288 \quad (41)$$

$$f^*_{BE} = -14762b^{18} - 285174b^{16} - 2659951b^{14} + 3029636b^{12} - 27622752b^{10} + 95326336b^8 - 226611968b^6 + 351556608b^4 - 321814528b^2 + 132120576 \quad (42)$$

Acknowledgment. We gratefully acknowledge support through the National Science Council of Taiwan, Republic of China under Grant NSC 98-2112-M-001-022-MY3 and the Asian Office of Aerospace Research & Development (AOARD) under Grant No. FA2386-09-1-4128. A.Z. also acknowledges financial support from the Basic Science Research Program through the National Research Foundation of Korea (NRF) funded by the Ministry of Education, Science and Technology (Grant No. 2009-0088557).

APPENDIX

The dimensionless coefficients for attractive part of tube−tube interaction potential are as the following

$$g_{AK}(b_1, b_2) = -[2\pi^2 {b_1}^4 {b_2}^4 \sum_{i,j=1\ldots3} \{p_{AK}\}_{ij} {b_1}^{2(i-1)} {b_2}^{2(j-1)}]/ [3(b_1b_2 + b_1 + b_2)^2(b_1b_2 - b_1 - b_2)^2(b_1b_2 + b_1 - b_2)^{5/2} \times (b_1b_2 + b_2 - b_1)^{5/2}] \quad (43)$$

$$g_{AE}(b_1, b_2) = -[2\pi^2 {b_1}^4 {b_2}^4 \sum_{i,j=1\ldots4} \{p_{AE}\}_{ij} {b_1}^{2(i-1)} {b_2}^{2(j-1)}]/ [3(b_1b_2 + b_1 + b_2)^3(b_1b_2 - b_1 - b_2)^3(b_1b_2 + b_1 - b_2)^{5/2} \times (b_1b_2 + b_2 - b_1)^{5/2}] \quad (44)$$

The matrices of integer coefficients $\{p_{AK}\}$ and $\{p_{AE}\}$ are

$$\{p_{AK}\} = \begin{bmatrix} 0 & 0 & -3 \\ 0 & 6 & -2 \\ -3 & -2 & 5 \end{bmatrix}$$

$$\{p_{AE}\} = \begin{bmatrix} 0 & 0 & 0 & 12 \\ 0 & 0 & -12 & -13 \\ 0 & -12 & 58 & -10 \\ 12 & -13 & -10 & 11 \end{bmatrix}$$

Analogically we write the dimensionless coefficients for repulsive part

$$g_{BK}(b_1, b_2) = -[\pi^2 {b_1}^{10} {b_2}^{10} \sum_{i,j=1\ldots12} \{p_{BK}\}_{ij} {b_1}^{2(i-1)} {b_2}^{2(j-1)}]/ [6300(b_1b_2 + b_1 + b_2)^8(b_1b_2 - b_1 - b_2)^8(b_1b_2 + b_2 - b_1)^{17/2} (b_1b_2 + b_2 - b_1)^{17/2}] \quad (45)$$

$$g_{BE}(b_1, b_2) = [\pi^2 {b_1}^{10} {b_2}^{10} \sum_{i,j=1\ldots13} \{p_{BE}\}_{ij} {b_1}^{2(i-1)} {b_2}^{2(j-1)}]/ [25200(b_1b_2 + b_1 + b_2)^9(b_1b_2 - b_1 - b_2)^9(b_1b_2 + b_1 - b_2)^{17/2} (b_1b_2 + b_2 - b_1)^{17/2}] \quad (46)$$

Matrices of integer coefficients $\{p_{BK}\}$ and $\{p_{BE}\}$ are placed in Tables 4 and 5, respectively.

The dimensionless coefficients for attractive and repulsive part of force are expressed as

$$f_{AK}(b_1, b_2) = [2\pi^2 {b_1}^4 {b_2}^4 \sum_{i,j=1\ldots5} \{q_{AK}\}_{ij} {b_1}^{2(i-1)} {b_2}^{2(j-1)}]/ [3(b_1b_2 + b_1 + b_2)^2(b_1b_2 - b_1 - b_2)^3(b_1b_2 + b_1 - b_2)^{7/2} \times (b_1b_2 + b_2 - b_1)^{7/2}] \quad (47)$$

$$f_{AE}(b_1, b_2) = -[4\pi^2 {b_1}^4 {b_2}^4 \sum_{i,j=1\ldots6} \{q_{AE}\}_{ij} {b_1}^{2(i-1)} {b_2}^{2(j-1)}]/ [3(b_1b_2 + b_1 + b_2)^3(b_1b_2 - b_1 - b_2)^3(b_1b_2 + b_1 - b_2)^{7/2} \times (b_1b_2 + b_2 - b_1)^{7/2}({b_1}^2{b_2}^2 - 2b_1b_2 - {b_1}^2 - {b_2}^2)] \quad (48)$$

$$f_{BK}(b_1, b_2) = [\pi^2 {b_1}^{10} {b_2}^{10} \sum_{i,j=1\ldots14} \{q_{BK}\}_{ij} {b_1}^{2(i-1)} {b_2}^{2(j-1)}]/ [5040(b_1b_2 + b_1 + b_2)^9(b_1b_2 - b_1 - b_2)^9 \times (b_1b_2 + b_1 - b_2)^{19/2}(b_1b_2 + b_2 - b_1)^{19/2}] \quad (49)$$

$$f_{BE}(b_1, b_2) = -[\pi^2 {b_1}^{10} {b_2}^{10} \sum_{i,j=1\ldots15} \{q_{BE}\}_{ij} {b_1}^{2(i-1)} {b_2}^{2(j-1)}]/ [5040(b_1b_2 + b_1 + b_2)^9(b_1b_2 - b_1 - b_2)^9(b_1b_2 + b_1 - b_2)^{19/2} \times (b_1b_2 + b_2 - b_1)^{19/2}({b_1}^2{b_2}^2 - 2b_1b_2 - {b_1}^2 - {b_2}^2)] \quad (50)$$

where

$$\{q_{AK}\} = \begin{bmatrix} 0 & 0 & 0 & 0 & 3 \\ 0 & 0 & 0 & -12 & 36 \\ 0 & 0 & 18 & -36 & -55 \\ 0 & -12 & -36 & 158 & -10 \\ 3 & 36 & -55 & -10 & 26 \end{bmatrix}$$

$$\{q_{AE}\} = \begin{bmatrix} 0 & 0 & 0 & 0 & 0 & -6 \\ 0 & 0 & 0 & 0 & 18 & -39 \\ 0 & 0 & 0 & -12 & -132 & 128 \\ 0 & 0 & -12 & 342 & -224 & -90 \\ 0 & 18 & -132 & -224 & 356 & -18 \\ -6 & -39 & 128 & -90 & -18 & 25 \end{bmatrix}$$

Matrices $\{q_{BK}\}$ and $\{q_{BE}\}$ are given in Tables 6 and 7, respectively.

TABLE 4. Matrix $\{p_{BK}\}$

0	0	0	0	0	0	0	0	0	0	0	0	−19530
	0	0	0	0	0	0	0	0	0	0	14490	−104685
		0	0	0	0	0	0	0	0	445410	−2015790	765744
			0	0	0	0	0	−1760850	7748055	−2248848	−1029636	
				0	0	0	2758140	−938280	−36368640	27011520	−1356976	
					0	−1437660	−31109610	114941568	−34271280	−35205136	5012854	
						52840620	−77089824	−172119744	193452624	−11269956	−5001276	
							360818280	−161478032	−132247830	47389620	1327256	
								295052744	−50123640	−24636352	1062586	
						Symmetry			54162000	−2009850	−786849	
										2858226	112076	
											18436	

TABLE 5. Matrix $\{p_{BE}\}$

0	0	0	0	0	0	0	0	0	0	0	0	0	177345
	0	0	0	0	0	0	0	0	0	0	0	976500	605220
		0	0	0	0	0	0	0	0	0	−9019710	28878780	−7265496
			0	0	0	0	0	0	18117540	−26421780	−43621536	16744920	
				0	0	0	0	4242735	−322255500	735299208	−256914792	−3437690	
					0	0	−66510360	827431080	−863979648	−1027666080	746908112	−43635920	
						104031900	−508237800	−2282192304	5778243552	−1895641688	−527458544	77409220	
							4923519552	−4510407600	−4710377296	4534092720	−365372760	−54614168	
								12018698404	−4283796976	−2131197060	690518216	8213905	
									5458820144	−809953328	−276097028	11278540	
						Symmetry				660421350	−23545932	−6367700	
											24951224	777760	
												114064	

TABLE 6. Matrix $\{q_{BK}\}$

0	0	0	0	0	0	0	0	0	0	0	0	0	15624
	0	0	0	0	0	0	0	0	0	0	0	−42840	755433
		0	0	0	0	0	0	0	0	0	−317520	4651668	−1248828
			0	0	0	0	0	0	2109744	−40861422	65362332	−11592924	
				0	0	0	0	−5380200	79474500	10951500	−192184440	44486040	
					0	0	6971832	28477575	−991483500	1506696660	−240160680	−50195242	
						0	−3356640	−318885336	2273850600	−1148679840	−2776597920	1286509520	−21785104
						492775164	−1357432104	−5600776440	10812253920	−1915609240	−1300087984	107776844	
							10893073968	−7839981360	−9567436112	7173492336	−138383496	−103517008	
								20757703300	−6144532400	−3892023180	951956720	33353705	
									8420997520	−1012896160	−459154660	9346988	
						Symmetry				973066230	−17001900	−8899384	
											37187456	1348304	
												155552	

TABLE 7. Matrix $\{q_{BE}\}$

0	0	0	0	0	0	0	0	0	−35469
	0	0	0	0	0	0	0	−124362	−1553454
		0	0	0	0	0	2159073	−24489990	4928091
			0	0	0	−7426692	104520780	−139540884	17567676
				0	0	8202411	84564396	−901760874	861398916	−110403234
					0	0	11375658	−1024742250	4609741500	−3041479980	−594533340	204320812
						0	0	−48259071	1921604958	−3163636875	−12201112980	16321695750	−3128825524	−103004658
							68216904	−1059904440	−11093841192	45974714520	−25761560400	−14217370384	6921793360	−196048368
								21368220468	−31611088152	−5535810954 0	87874942896	−17650761720	−4488366288	380618007
									131005821528	−71790032408	−50711821008	34135947792	−1350545098	−270248958
										128236620500	−32263986000	−13793389735	3110622970	63736407
											33152425140	−3602984700	−1197711564	24929412
						Symmetry						2709914346	−49166500	−17323848
													77206912	2281392
														236192

REFERENCES AND NOTES

1. Anantram, M. P.; Léonard, F. Physics of Carbon Nanotube Electronic Devices. *Rep. Prog. Phys.* **2006**, *69*, 507–561.
2. Zhbanov, A. I.; Sinitsyn, N. I.; Torgashov, G. V. Nanoelectronic Devices Based on Carbon Nanotubes. *Radiophys. Quantum Electron.* **2004**, *47*, 435–452.
3. Kim, P.; Lieber, C. M. Nanotube Nanotweezers. *Science* **1999**, *286*, 2148–2150.

4. Dequesnes, M.; Rotkin, S. V.; Aluru, N. R. Calculation of Pull-in Voltages for Carbon Nanotube-Based Nanoelectromechanical Switches. *Nanotechnology* **2002**, *13*, 120–131.
5. Cumings, J.; Zettl, A. Low-Friction Nanoscale Linear Bearing Realized from Multiwall Carbon Nanotubes. *Science* **2000**, *289*, 602–604.
6. Rueckes, T.; Kim, K.; Joselevich, E.; Tseng, G. Y.; Cheung, C.-L.; Lieber, C. M. Carbon Nanotube-Based Nonvolatile Random Access Memory for Molecular Computing. *Science* **2000**, *289*, 94–97.
7. Maslov, L. Concept of Nonvolatile Memory Based on Multiwall Carbon Nanotubes. *Nanotechnology* **2006**, *17*, 2475–2482.
8. Kang, J. W.; Jiang, Q.; Hwang, H. J. A Double-Walled Carbon Nanotube Oscillator Encapsulating a Copper Nanowire. *Nanotechnology* **2006**, *17*, 5485–5490.
9. Girifalco, L. A.; Lad, R. A. Energy of Cohesion, Compressibility, and the Potential Energy Functions of the Graphite System. *J. Chem. Phys.* **1956**, *25*, 693–697.
10. Girifalco, L. A. Molecular Properties of C_{60} in the Gas and Solid Phases. *J. Phys. Chem.* **1992**, *96*, 858–861.
11. Rey, C.; García-Rodeja, J.; Gallego, L. J.; Alonso, J. A. Clusters and Layers of C_{60} Molecules Supported on a Graphite Substrate. *Phys. Rev. B* **1997**, *55*, 7190–7197.
12. Dong, L.; Arai, F.; Fukuda, T. Destructive Constructions of Nanostructures with Carbon Nanotubes through Nanorobotic Manipulation. *IEEE Trans. Mechatron.* **2004**, *9*, 350–357.
13. Girifalco, L. A.; Hodak, M.; Lee, R. S. Carbon Nanotubes, Buckyballs, Ropes, and a Universal Graphitic Potential. *Phys. Rev. B* **2000**, *62*, 13104–13110.
14. Sun, C.-H.; Yin, L.-C.; Li, F.; Lu, G.-Q.; Cheng, H.-M. Van der Waals Interactions between Two Parallel Infinitely Long Single-Walled Nanotubes. *Chem. Phys. Lett.* **2005**, *403*, 343–346.
15. Cao, D.; Wang, W. Interaction between Two Single-Walled Carbon Nanotubes Revisited: Structural Stability of Nanotube Bundles. *Chem. Eng. Sci.* **2007**, *62*, 6879–6884.
16. Popescu, A.; Woods, L. M.; Bondarev, I. V. Simple Model of van der Waals Interactions between Two Radially Deformed Single-Wall Carbon Nanotubes. *Phys. Rev. B* **2008**, *77*, 115443.
17. Rotkin, S. V.; Hess, K. Many-Body Terms in van der Waals Cohesion Energy of Nanotubes. *J. Comput. Electron.* **2002**, *1*, 323–326.
18. Saito, R.; Matsuo, R.; Kimura, T.; Dresselhaus, G.; Dresselhaus, M. S. Anomalous Potential Barrier of Double-Wall Carbon Nanotube. *Chem. Phys. Lett.* **2001**, *348*, 187–193.
19. Baowan, D.; Hill, J. M. Force Distribution for Double-Walled Carbon Nanotubes and Gigahertz Oscillators. *Z. Angew. Math. Phys.* **2007**, *2007*, 857–875.
20. Sun, C.-H.; Lu, G.-Q.; Cheng, H.-M. Simple Approach to Estimating the van der Waals Interaction between Carbon Nanotubes. *Phys. Rev. B* **2006**, *73*, 195414.
21. Zheng, Q.; Liu, J. Z.; Jiang, Q. Excess van der Waals Interaction Energy of a Multiwalled Carbon Nanotube with an Extruded Core and the Induced Core Oscillation. *Phys. Rev. B* **2002**, *65*, 245409.
22. London, F. Zur Theorie und Systematik der Molekularkräfte. *Z. Phys.* **1930**, *63*, 245–279.
23. Kostov, M. K.; Cole, M. W.; Lewis, J. C.; Diep, P.; Johnson, J. K. Many-Body Interactions among Adsorbed Atoms and Molecules within Carbon Nanotubes and in Free Space. *Chem. Phys. Lett.* **2000**, *332*, 26–34.
24. Gatica, S. M.; Cole, M. W.; Velegol, D. Designing van der Waals Forces between Nanocolloids. *Nano Lett.* **2005**, *5*, 169–173.
25. Gatica, S. M.; Calbi, M. M.; Cole, M. W.; Velegol, D. Three-Body Interactions Involving Clusters and Films. *Phys. Rev. B* **2003**, *68*, 205409.
26. Axilrod, B. M.; Teller, E. Interaction of the van der Waals Type Between Three Atoms. *J. Chem. Phys.* **1943**, *11*, 299–300.
27. Muto, Y. Force between Nonpolar Molecules. *Proc. Phys.-Math. Soc. Jpn.* **1943**, *17*, 629–631.
28. Casimir, H. B. G. On the Attraction of Two Perfectly Conducting Plates. *Proc. K. Ned. Akad. Wet.* **1948**, *51*, 793–795.
29. Casimir, H. B. G.; Polder, D. The Influence of Retardation on the London−van der Waals Forces. *Phys. Rev.* **1948**, *73*, 360–372.
30. Lifshitz, E. M. The Theory of Molecular Attractive Forces between Solids. *Soviet Phys. JETP* **1956**, *2*, 73–83.
31. Dzyaloshinskii, I. E.; Lifshitz, E. M.; Pitaevskii, L. P. The General Theory of van der Waals Forces. *Adv. Phys.* **1961**, *10*, 165–209.
32. Blagov, E. V.; Klimchitskaya, G. L.; Mostepanenko, V. M. van der Waals Interaction Between a Microparticle and a Single-Walled Carbon Nanotube. *Phys. Rev. B* **2007**, *75*, 235413.
33. Pacheco, J. M.; Ramalho, J. P. P. First-Principles Determination of the Dispersion Interaction between Fullerenes and Their Intermolecular Potential. *Phys. Rev. Lett.* **1997**, *79*, 3873–3876.
34. Grimme, S. Semiempirical Hybrid Density Functional with Perturbative Second-Order Correlation. *J. Chem. Phys.* **2006**, *124*, 034108.
35. Schwabe, T.; Grimme, S. Double-Hybrid Density Functionals with Long-Range Dispersion Corrections: Higher Accuracy and Extended Applicability. *Phys. Chem. Chem. Phys.* **2007**, *9*, 3397–3406.
36. Grimme, S.; Antony, J.; Schwabe, T.; Mück-Lichtenfeld, C. Density Functional Theory with Dispersion Corrections for Supramolecular Structures, Aggregates, and Complexes of (Bio)Organic Molecules. *J. Chem. Phys.* **2007**, *5*, 741–758.
37. Bondarev, I. V.; Lambin, P. Van der Waals Coupling in Atomically Doped Carbon Nanotubes. *Phys. Rev. B* **2005**, *72*, 035451.
38. Girifalco, L. A.; Hodak, M. Van der Waals Binding Energies in Graphitic Structures. *Phys. Rev. B* **2002**, *65*, 125404.
39. Popescu, A.; Woods, L. M.; Bondarev, I. V. A Carbon Nanotube Oscillator as a Surface Profiling Device. *Nanotechnology* **2008**, *19*, 435702.
40. Wang, X.; Sun, B.; Yang, H. K. Stability of Multiwalled Carbon Nanotubes under Combined Bending and Axial Compression Loading. *Nanotechnology* **2006**, *17*, 815–823.
41. Dong, K.; Wang, X. Wave Propagation in Carbon Nanotubes under Shear Deformation. *Nanotechnology* **2006**, *17*, 2773–2782.
42. Ruoff, R. S.; Tersoff, J.; Lorents, D. C.; Subramohey, S.; Chan, B. Radial Deformation of Carbon Nanotubes by van der Waals Forces. *Nature* **1993**, *364*, 514–516.
43. Hertel, T.; Walkup, R. E.; Avouris, P. Deformation of Carbon Nanotubes by Surface van der Waals Forces. *Phys. Rev. B* **1998**, *58*, 13870–13873.
44. Abrams, Z. R.; Hanein, Y. Radial Deformation Measurements of Isolated Pairs of Single-Walled Carbon Nanotubes. *Carbon* **2007**, *45*, 738–743.
45. Jiang, Y. Y.; Zhou, W.; Kim, T.; Huang, Y.; Zuo, J. M. Measurement of Radial Deformation of Single-Wall Carbon Nanotubes Induced by Intertube van der Waals Forces. *Phys. Rev. B* **2008**, *77*, 153405.
46. Amovilli, C.; March, N. H. Long-Range Forces Between C Nanotubes and between C Cages: Some Polarizability Bounds and Scaling Approximations Yielding Interaction Energies at Intermediate Separations. *Carbon* **2005**, *43*, 1634–1642.
47. Abramowitz, M.; Stegun, I. A. In *Handbook of Mathematical Functions*; Dover Publications: New York, 1964; Chapter 17.
48. Hancock, H. *Lectures on the Theory of Elliptic Functions*; J. Wiley & Sons: New York, 1910.
49. Greenhill, A. G. *The Applications of Elliptic Functions*; Macmillan: New York, 1892.
50. King, L. V. *On the Direct Numerical Calculation of Elliptic Functions and Integrals*; Cambridge University Press: Cambridge, U.K., 1924.